

## **Precipitation extremes and the impacts of climate change on stormwater infrastructure in Washington State**

Eric A. Rosenberg<sup>1</sup>, Patrick W. Keys<sup>1</sup>, Derek B. Booth<sup>1,2</sup>, David Hartley<sup>3</sup>, Jeff Burkey<sup>4</sup>,  
Anne C. Steinemann<sup>1,5</sup>, and Dennis P. Lettenmaier<sup>1</sup>

1) Department of Civil and Environmental Engineering, University of Washington,  
Seattle, WA 98195

2) Stillwater Sciences, Santa Barbara, CA 93102

3) Northwest Hydraulic Consultants, Seattle, WA 98188

4) King County Water and Land Resources Division, Seattle, WA 98104

5) Evans School of Public Affairs, University of Washington, Seattle, WA 98195

## **Abstract**

Stormwater management facilities are important elements of the civil infrastructure that can be sensitive to climate change, particularly to precipitation extremes that generate peak runoff flows. The design and anticipated performance of stormwater infrastructure is based on either the presumed characteristics of a “design rainstorm” or the continuous simulation of streamflow driven by a time series of precipitation. Under either approach, a frequency distribution of precipitation is required, either directly or indirectly, together with an underlying assumption that the probability distribution of precipitation extremes is statistically stationary. This assumption, and hence both approaches, are called into question by climate change. We therefore examined both historical precipitation records and simulations of future rainfall to evaluate past and prospective changes in the probability distributions of precipitation extremes across Washington State. The historical analyses were based on hourly precipitation records for the time period 1949–2007 from weather stations surrounding three major metropolitan areas of the state: the Puget Sound region (including Seattle, Tacoma, and Olympia), the Vancouver (WA) region (including Portland, OR), and the Spokane region. Changes in future precipitation were simulated using two runs of the Weather Research and Forecast regional climate model (RCM) for the time periods 1970–2000 and 2020–2050, statistically downscaled from the ECHAM5 and CCSM3 Global Climate Model and bias-corrected against the SeaTac Airport rainfall record. Downscaled and bias-corrected hourly precipitation sequences were then used as input to the HSPF hydrologic model to simulate streamflow in two urban watersheds in central Puget Sound. Few statistically significant changes in extreme precipitation were observed in the historical records, with the possible exception of the Puget Sound. RCM simulations generally indicate increases in extreme rainfall

magnitudes throughout the state, but the range of projections is too large to predicate engineering design, and actual changes could be difficult to distinguish from natural variability. Nonetheless, the evidence suggests that drainage infrastructure designed using mid-20th century rainfall records may be subject to a future rainfall regime that differs from current design standards.

## **1. Introduction**

Infrastructure is commonly defined as the various components of the built environment that support modern society (e.g., Choguill 1996; Hanson 1984). These encompass utilities, transportation systems, communication networks, water systems, and other elements that include some of the most critical underpinnings of civilization. Thus even modest disruptions to infrastructure can have significant effects on daily life, and any systematic change in the frequency or intensity of those disruptions could have profound consequences for economic and human well-being.

The elements of Washington's urban infrastructure are not equally vulnerable to weather conditions or climate regime, however, and several components (energy, water supply, and coastal facilities) are the subject of other reports in this volume (Hamlet et al. 2009, this report; Huppert et al. 2009, this report; Vano et al. 2009a, b, this report). Prior studies have considered the vulnerability of these and other infrastructure elements, and the daily news provides frequent examples of those elements of our Northwest cities that are most vulnerable to the vagaries of even present-day fluctuations in weather. The

Chehalis River floods in December 2007, for example, resulted in the closure of Interstate 5, the state's major north–south transportation artery, for four days at an estimated cost of over \$18M (WSDOT 2008).

In this paper, we focus on one element of the civil infrastructure, stormwater management facilities in urban areas. The relationship of this sector to climate, and particularly to precipitation extremes on which much of its facility design is based, is clear. Recent improvements in the ability to downscale the projections of global climate models to the local scale (Salathé et al. 2005) have made feasible the preliminary evaluation of climate change impacts on the spatially heterogeneous, rapidly fluctuating behavior of urban stormwater. Consequences of inadequate stormwater facilities can be severe, but adaptation strategies are available and relatively straightforward if anticipated well in advance (Kirschen 2004; Larsen 2007; Shaw 2005).

Historical management goals for urban stormwater have emphasized safe conveyance, with more recent attention also being given to the consequences of increased streamflows on the physical and biological integrity of downstream channels (Booth and Jackson 1997). Urbonas and Roesner (1993) classify drainage systems into two categories – minor, consisting of the roadside swales, gutters, and sewers typically designed to convey runoff events of 2- or 5-year return periods, and major, which include the larger flood control structures designed to manage 50- or 100-year events. While design events can be based on direct observations of runoff, they are more commonly based on precipitation events with equivalent likelihoods of occurrence, due to the limited availability of runoff observations in urban areas. Hence, while we give some consideration to modeled trends

in runoff, the focus of this paper is on the precipitation events from which they result, and specifically those events of 1-hour duration (since many of the smaller watersheds have times of concentration of 1 hour or less) and 24-hour duration (which is that most commonly used for purposes of design).

It is worth noting that more complicated phenomena with implications for stormwater management, such as rain-on-snow events, are also subject to the effects of a changing climate. We do not consider trends in these phenomena, however, since our modeling approach is not well-calibrated for such conditions, which are not necessarily significant in the lowland urban areas that are the focus of our study. Nor do we consider changing patterns of development, which may also considerably impact runoff magnitudes, but are not related to climatic factors. Nonetheless, future changes in climate that may alter precipitation intensity or duration would likely have consequences for urban stormwater discharge, particularly where stormwater detention and conveyance facilities were designed under assumptions that may no longer be correct. The social and economic impact of increasing the capacity of undersized stormwater facilities, or the disabling of key assets because of more severe flooding, could be substantial.

This study thus addresses the following questions:

- What are the historical trends in precipitation extremes across Washington State?
- What are the projected trends in precipitation extremes over the next 50 years in the state's urban areas?

- What are the likely consequences of future changes in precipitation extremes on urban stormwater infrastructure?

## **2. Background**

Despite the inherent challenges in characterizing changes in extreme rainfall events, a number of studies have either assessed historical trends in precipitation metrics or investigated the vulnerability of stormwater infrastructure under a changing climate, as described below.

### **2.1 Historical trends in precipitation extremes**

Several studies have evaluated past trends in rainfall extremes of various durations, mostly at national or global scales. Karl and Knight (1998) found a 10% increase in total annual precipitation across the contiguous United States since 1910, and attributed over half of the increase to positive trends in both frequency and intensity in the upper ten percent of the daily precipitation distribution. Kunkel et al. (1999) found a national increase of 16% from 1931-96 in the frequency of 7-day extreme precipitation events, although no statistically significant trend was found specifically for the Pacific Northwest. A follow-up study that employed data extending to 1895 (Kunkel et al. 2003) generally reinforced these findings, but noted that frequencies for some return periods were nearly as high at the beginning of the 20th century as they were at the end, suggesting that natural variability could not be discounted as an important contributor to the observed trends.

Groisman et al. (2005) analyzed precipitation data over half of the global land area and found “an increasing probability of intense precipitation events for many extratropical regions including the United States.” They defined intense precipitation events as the upper 0.3% of daily observations, and used three model simulations with transiently increasing greenhouse gases to offer preliminary evidence that these trends are linked to global warming. Pryor et al. (2009) analyzed eight metrics of precipitation in century-long records throughout the contiguous USA, finding that statistically significant trends generally indicated increases in intensity of events above the 95th percentile, although few of these were located in Washington State. However, Madsen and Figdor (2007), in a study that systematically analyzed trends from 1948 to 2006 by both state and metropolitan area, found a statistically significant increase of 30% in the frequency of extreme precipitation in Washington, and of 45% in the Seattle-Tacoma-Bremerton area. Interestingly, however, trends in neighboring states were widely incongruent, with a statistically significant *decrease* of 14% in Oregon and a non-significant increase of 1% in Idaho.

While these studies provide useful impressions of general trends in precipitation extremes, their results are not applicable to infrastructure design, which requires estimates of the distributions of extreme magnitudes instead of, for example, the number of exceedances of a fixed threshold. Relatively few such approaches have been explored to date, with the exception of Fowler and Kilsby (2003), which used regional frequency analysis to determine changes in design storms of 1, 2, 5, and 10 day durations from 1961

to 2000 in the United Kingdom. We take this approach one step further and analyze changes in design storms of sub-daily durations, as discussed in Section 3.

## **2.2 Future projections and adaptation options**

Only a few previous studies have evaluated the vulnerability of stormwater infrastructure to climate change, with considerable variation in their methodologies. Denault et al. (2002) assessed urban drainage capacity under future precipitation for a 440-ha (1080-ac) urban watershed in North Vancouver, Canada. Observed trends of precipitation intensity and magnitude for the period 1964–1997 were projected statistically to infer the magnitude of design storms in 2020 and 2050, and the consequences for urban discharges were modeled using the SWMM hydrologic model<sup>1</sup>. They evaluated only the potential impacts on pipe capacity, finding that flow increases were sufficiently small that few if any new problems were likely to be created. They also observed that any given watershed has unique characteristics that affect its ability to accommodate specific impacts, thus emphasizing the importance of site-specific evaluation. They also recognized that uniform climate changes could produce varying levels of impact on any individual municipality, because of differences in topography, watershed size, level of development, and(or) existing infrastructure drainage capacity.

Waters et al. (2003) evaluated how a small (23 ha [58 ac]) urban watershed in the Great Lakes region (Burlington, Ontario) would be affected by a 15% increase in rainfall depth

---

<sup>1</sup> <http://www.epa.gov/ednrmrl/models/swmm/>

and intensity. This increase was presumed from a literature review and prior analysis of other nearby catchments. Their study emphasized the adaptive measures that could be taken to absorb the increased rainfall, and they evaluated the efficacy of alternative adaptations to projected flow increases using SWMM. Their recommended measures included downspout disconnection (50% of connected roofs), increased depression storage (by 45 m<sup>3</sup>/impervious hectare), and increased street detention storage (by 40 m<sup>3</sup>/impervious hectare).

Shaw et al. (2005) also emphasized the consequences of presumed increases in precipitation on flooding of stormwater systems, while relying on relatively simplistic projections of future precipitation. They defined low, medium and high climate-change scenarios, based on projections of temperature increase, and translated those temperature increases into linear increases in 24-hour rainfall events. Consequences on stormwater capacity for a small urban watershed in central New Zealand (the Wairau Valley watershed in North Shore City, North Island), using both event-based and continuous hydrologic models, were then evaluated for inadequate infrastructure capacity.

Watt et al. (2003) examined the multiple impacts that climate change could have on stormwater design and infrastructure in Canada, suggesting adaptive measures for urban watersheds with their associated advantages, disadvantages, and estimated costs. The authors also examined two case studies of adapting stormwater infrastructure to climate change; one was the study of Waters et al. (2003) and the other was a study of a residential area in urban Ottawa. They offered a useful qualitative rating system to

compare the environmental, social, and aesthetic implications of different structural solutions to stormwater runoff management.

Crabbé and Robin (2006) studied the need for institutional “adaptation” to be better able to respond and adapt to climate change. The authors focused on the bureaucracies of Canada and the financial and physical responsibility that local municipalities will need to bear in adapting infrastructure to climate change. The review considered the institutional costs for preparing water-resources infrastructure for climate change, and the potential increases in both revenues and expenditures for local and regional governments. It also acknowledged institutional barriers, such as a lack of skilled scientists, over-dependence on engineering consultants, and reliance on management-by-crisis rather than long-term management and planning. The study offered potential approaches to solve these impediments, including easily understandable climate-change reporting, increased citizen participation, and financial assistance from regional governments.

These prior studies provide a good methodological starting point for identifying the most likely consequences of climate change on stormwater infrastructure, along with an initial list of potentially useful adaptation measures. Like those presented in Section 2.1, however, their greatest shortcoming uniformly lies in their rudimentary characterization of the precipitation regimes that drive the responses (see also Kirschen et al. 2004; Trenberth et al. 2003). Our report seeks to bridge this gap between presumptive (but poorly quantified) future climate change and the acknowledgment that infrastructure adaptation is generally less costly and disruptive if necessary measures are undertaken well in advance of anticipated changes.

We have approached this task both by analyzing the variability in historical precipitation extremes across Washington State and by utilizing regional climate model results, now available at a higher resolution than previously possible, to characterize future projections of precipitation extremes. We processed these results in a bias-correction and statistical-downscaling procedure to drive a continuous hydrologic model for prediction of urban streamflows in one region of the state, the central Puget Lowland. These results have allowed a preliminary evaluation of the implications of simulated precipitation extremes for urban drainage and urban flooding.

### **3. Historical precipitation analysis**

As a precursor to investigating potential changes in future precipitation extremes as simulated by climate models, we examined whether such changes might already be occurring in the three major urban areas of Washington State. Three different analyses were applied to historical rainfall records, beginning in 1949, to look for such trends: (1) regional frequency analysis, (2) precipitation event analysis, and (3) exceedance-over-threshold analysis. In the *regional frequency analysis*, we used a technique adapted from the regional L-moments method of Hosking and Wallis (1997) to evaluate changes in rainfall extremes over the period 1956–2005 for a wide range of frequencies and durations. The *precipitation event analysis* used a method adapted from Karl and Knight (1998) to determine trends in annual precipitation event frequency and intensity, based on the occurrence of individual rainfall “events” of presumed one-day duration. Finally, the

*exceedance-over-threshold analysis* examined the number of exceedances above a range of threshold values for the depth of precipitation, also on the basis of one-day rainfall events.

### **3.1 Regional frequency analysis**

The precipitation frequency analysis (sometimes referred to as the index-flood approach) analyzed the annual maximum series for aggregates of hourly precipitation ranging from one hour to ten days for the three major urban areas in Washington State: the Puget Sound region (including Seattle, Tacoma, and Olympia), the Vancouver region (including Portland, OR), and the Spokane region. The approach entails fitting a frequency distribution to time series of annual precipitation maxima from a set of *multiple* stations within a region, rather than fitting the data from a single station to an individual distribution. The strength of this method is in the regionalization, allowing for a larger sampling pool of data points and a more robust fit to the probability distribution, resulting in estimates of extreme quantiles that are considerably less variable than at-site estimates (e.g., Lettenmaier et al. 1987). Data originated from National Climatic Data Center (NCDC) hourly precipitation archives and were extracted using commercial software provided by Earth Info, Inc. Stations selected for the analysis are shown in Figure 1 and listed in Table 1. The minimum requirement for inclusion was a reported period of record of 40 years. Years with more than 40% missing data in the fall and winter months were removed from the analysis, since precipitation events during these two seasons have the highest probabilities of being annual maxima, and so the precipitation that was recorded could misrepresent that year's true annual maximum.

A basic premise of regional frequency analysis is that all sites within a region can be described by a common probability distribution after site data are divided by their at-site means. These common probability distributions are referred to as regional growth curves. Design storms at individual sites can then be calculated by reversing the process, multiplying the regional growth curves by at-site means. The approach provides the advantage of greater sample sizes, which allow for more reliable estimation of long return-period events even if individual records are otherwise too short.

Annual maximum precipitation depths for multiple durations (1, 2, 3, 6, 12, and 24 hours; and 2, 5, and 10 days) were identified for each station and combined into pools in order to calculate regional L-moment parameters (Fowler and Kilsby 2003; Hosking and Wallis 1997). These parameters were then used to fit data to Generalized Extreme Value (GEV) distributions and to generate regional growth curves. We then analyzed for any historical trends in precipitation by dividing the precipitation record from each region into two 25-year periods (1956–1980 and 1981–2005). We investigated a finer division of the data into five 10-year periods, but the results were statistically inconclusive and so are not reported here. For each of the two 25-year periods, design storm magnitudes were determined at Seattle Tacoma (SeaTac), Spokane, and Portland International Airports based on the regional growth curves and the means at those stations. A bootstrap method (Efron 1979), whereby one year of record was removed at a time and growth curves refitted, was used to provide uncertainty bounds about the GEV distributions. Changes in design storm magnitudes were determined by comparing the distributions from each period. Statistical significance for differences in distributions was found using the

Komolgorov-Smirnov test, for differences in means using the Wilcoxon rank-sum test, and for trends in the entire time series using the Mann-Kendall test, all at a two-sided significance level of 0.05.

The summarized results (Table 2) present the average of changes in design storm magnitudes across all recurrence intervals (from 1.01-yr through 100-yr), which generally is about the same magnitude of change seen in the 2-year events. Changes at SeaTac were consistently positive, with the greatest increases seen at the 24-hour and 2-day durations. Changes at Spokane were mixed, while changes at Vancouver were mostly negative, with the notable exception of the 1- and 24-hour durations. None of the changes were found to be statistically significant, however, with the exception of the 2-day and (possibly) 24-hour durations at SeaTac.

A breakdown of changes by return period is provided for the 1- and 24-hour durations in Table 3, so chosen because of their relevance to urban stormwater infrastructure as indicated in Section 1. Included in the table are estimated return periods of the 1981–2005 events that are equal in magnitude to the 1956–1980 events having the return periods indicated in the first column. Rainfall frequency curves that illustrate the changes in 1- and 24-hour durations listed in Table 3 are shown in Figure 2. Shaded regions represent uncertainty bounds as determined by bootstrapping the historical data but do not necessarily indicate statistical significance or nonsignificance in changes.

In summary, the last half-century has seen significant increases in extreme precipitation in the Puget Sound region, with much more ambiguous changes in other parts of the state.

For changes in the 24-hour duration at SeaTac, which come closest to attaining statistical significance, the largest change is seen at the 50-year return period, which increases in magnitude by 37%. Thus, what was a 50-year storm (i.e., having a 2% (1/50) chance of occurring in any given year) from 1956–1980 became an 8.4-year storm (i.e., having a 12% (1/8.4) chance of occurring in any give year) from 1981–2005, and is thus about six times as likely to occur. These results suggest that urban stormwater systems in the Puget Sound region probably have already experienced substantially increased peak discharges over the past half-century.

### **3.2 Precipitation event analysis**

In addition to changes in extreme precipitation frequency distributions, it is also useful to recognize any trends in total annual precipitation, and to determine whether such trends are due to changes in storm frequency, storm intensity, or both. An analysis to determine these trends was performed on the NCDC precipitation data by adapting the method of Karl and Knight (1998), which requires a continuous precipitation record for its application. Thus, we used the single station in each of the urban areas analyzed in the previous section with the most complete record—the airport gauges at Seattle-Tacoma, Spokane, and Portland. Each had a common period of record from January 1, 1949 to December 31, 2007, for a total of 59 years.

The central concept in this approach is that once trends in total annual precipitation are determined, the relative influence of changes in event *frequency* and changes in event

*intensity* can be identified. Trends in event frequency can be determined by defining a precipitation event as any nonzero accumulation over a specified time interval, and tallying their number in each period. The remainder of the trends in total annual precipitation can then be attributed to the trends in event intensity, defined as the amount of precipitation in a given event.

This approach provides the additional advantage of determining whether changes were due to trends in light precipitation events, trends in heavy precipitation events, or both. This is a consequence of breaking down each rainfall record into multiple intervals based on event magnitude. For this study, an event was defined as any measurable precipitation over a 24-hour period (midnight-to-midnight), although this requires an assumption that any day with nonzero precipitation is a single “event” (even though a single storm may have spanned the division between two days while lasting less than 24 hours, or there could have been two events in one day separated by one or more hours of no rain).

The analysis is performed by first calculating both the total precipitation and the number of “events” for each year (as defined above), ranking those events from lowest to highest, and dividing them into 20 class intervals that each contain 1/20 of the total number of events for that year. Thus the first class interval is assigned the 5% of events with the lowest daily totals, the second class interval is assigned the 5% of events with the next lowest daily totals, etc. For each class, the average long-term precipitation per event (event intensity) is then calculated, and the trend in precipitation due to the trend in event frequency is calculated as:

$$b_e = \overline{P_e} b_f,$$

where  $\overline{P_e}$  is the average long-term event intensity and  $b_f$  is the percent change in the frequency of events, as determined by the slope of the linear regression line through a scatter plot of number of events vs. year. The trend in precipitation due to the trend in the annual intensity of events is then calculated as a residual using the expression:

$$b_i = b - b_e,$$

where  $b$  is the percent change in total precipitation, as determined by the slope of the linear regression line through a scatter plot of total precipitation versus year. Median and highest precipitation events are calculated regardless of class for each year, and trends again are determined by the slopes of their respective regression lines. All trends are divided by average values and multiplied by the 59-year period of analysis.

Results of the analysis are summarized at the annual level for all three stations in Table 4. Trends were tested for significance using the Mann-Kendall test at a two-sided significance level of 0.05. Although none were found to be significant, trends were consistently negative for total precipitation and event frequency, and mostly negative for event intensity. As an example, at Spokane, total annual precipitation has decreased by 13.0% since 1949; 11.9% of this decrease was due to a decrease in event frequency, and the remaining 1.1% of this decrease was due to a decrease in event intensity. Trends in

median event intensity were mixed, however, while trends in maximum event intensity were mostly positive.

Distributions of annual trends by class are presented in Figure 3, with the class interval containing the smallest 5% of events to the left of each graph and the class interval containing the largest 5% of events (i.e., extreme events) to the right. The sums of the trends in each class equal the cumulative values reported in Table 4. At SeaTac, for example, despite mostly negative trends in intensity for the lowest 19 class intervals, a relatively large increasing trend in the intensity of the extreme class interval causes the cumulative trend for intensity to be slightly positive. A closer inspection of the data behind these results at SeaTac reveals that 3 of the 4 highest 1-day totals since 1949 have occurred in the last five years.

### **3.3 Exceedance-over-threshold analysis**

In addition to the regional frequency and precipitation event analyses, examining the number of events exceeding a given threshold (e.g., 0.1 in, 0.2 in, etc.) throughout a precipitation record can provide more detailed information on historical changes in frequency. Such an “exceedance-over-threshold” analysis, distinct from a peak-over-threshold approach which then uses the magnitudes of these events to estimate design storms, was conducted for the three stations examined in Section 3.2. All recorded nonzero daily precipitation totals were again treated as single events. Trends were determined by linear regression and expressed as a percentage of the average annual

number of exceedances over the 59-year period. The Mann-Kendall test was again employed to test for statistical significance at a two-sided significance level of 0.05.

As found in the precipitation event analysis, trends in the frequencies of exceedance (Table 5) were negative across all thresholds, suggesting a modest overall decrease in the number of rain events consistent with the decrease in event frequency found in Section 3.2. Statistically significant trends were found for events exceeding several of the thresholds, such as 0.2” at SeaTac displaying a 15% decrease over the 59-year period. This particular analysis does not consider exceedances of thresholds larger than 0.5” due to the small numbers of these that occur annually, which preclude any meaningful interpretation of trends regarding more extreme events.

### *Summary*

Although the three components of the historical precipitation analysis demonstrate a high degree of variability in both time and space, a few patterns emerge from these analyses:

1. Results of the regional frequency analysis, which evaluated annual maxima, indicate consistently positive changes in precipitation extremes in the Puget Sound region, with significant increases occurring in 24-hour and 2-day storms. Results from Spokane and Portland-Vancouver, however, are more variable, and none of the changes in these regions are statistically significant.
2. Trends in the precipitation event and peak-over-threshold analyses are consistently negative in all three regions for both total precipitation and event frequency, though most are nonsignificant.

3. Overall, the rainfall record of the Puget Sound region suggests that total annual precipitation has decreased, but the magnitude of large, low-frequency events has increased across all durations. Spokane displays a similar pattern in total annual precipitation, but a less pronounced pattern in changes in event magnitude, which vary in sign depending on storm duration. Portland–Vancouver, in contrast, displays decreases in both total annual precipitation and extreme event magnitudes at most durations. The only statistically significant change with relevance to stormwater infrastructure, however, is the increase in magnitude of 24-hour extremes in the Puget Sound region.

#### **4. Modeled trends in future extreme precipitation**

Urban watersheds are small and commonly provide rapid surface flow paths for runoff, thus responding very quickly to even short-duration events (Leopold 1968). Their discharge records reflect the influence of individual storm cells and localized bands of high-intensity rainfall, which can sometimes produce runoff responses that vary greatly over just a few kilometers (Gerstel et al. 1997). Thus the raw output from Global Climate Models (GCMs), on which most assessments of future climate are based, is not directly useable because the model grid resolution (100s of km) is much too coarse. For Washington State, however, two regional climate model simulations were performed to downscale the GCM output into hourly precipitation with spatial resolutions of 20 and 36 km (Leung et al. 2006; Salathé et al. 2008; Salathé et al. 2009, this report). Although these spatial and temporal scales are not ideal for capturing the behavior of urban runoff

response, the use of nested model simulations to estimate annual maximum series of precipitation (as opposed to peak-over-threshold extremes only) represents a significant advance in our ability to understand precipitation at the local scales at which watersheds respond to intense rainfall.

The two regional climate model (RCM) simulations used here and described in Salathé et al. (2009, this report) use different IPCC (2007) GCM outputs as their boundary conditions. Because the RCM runs are linked via their boundary conditions to different GCMs that each predict future climate differently, and that also use slightly different global emissions scenarios, it is expected that they will also differ in their projections of future climate. Ideally, a multimodel ensemble at the regional scale, paralleling that being used for regional hydrologic analysis (e.g., Vano et al. 2009a, b, this report), would be available for our analyses. At present, however, this strategy is not computationally feasible (each RCM simulation required several months of computer time). Thus the results presented here can offer a sense of the likely direction and general magnitude of future changes in precipitation extremes, but reducing their substantial uncertainties must await additional RCM simulations that can be linked to the many other GCMs presently in existence.

#### **4.1 RCM summary**

The two global climate models (GCMs) that were used to provide boundary conditions for the RCM simulations were the Community Climate System Model version 3.0

(CCSM3) under the A2 emissions scenario, and the Max Planck Institute's ECHAM5 under the A1B emissions scenario (Table 6). During the first half of the 21<sup>st</sup> century, atmospheric CO<sub>2</sub> concentrations are similar in both the A2 and the A1B emissions scenarios, and so differences in the RCM simulation results are most likely expressions of differences in the GCMs. Slight differences in spatial resolution may also influence these results, but they have not been systematically explored to date. Both CCSM3 and ECHAM5 are considered to be in the middle of the range of existing GCMs in their projections of precipitation for the Pacific Northwest (Mote et al. 2005).

The RCM employed to downscale both GCMs was the Advanced Research Weather Research and Forecasting (WRF) mesoscale climate model. The CCSM3/A2 WRF simulation was performed on a grid spacing of 20 km, while the ECHAM5/A1B WRF simulation had a grid spacing of 36 km. Both simulations were used to simulate hourly precipitation data for the time periods 1970–2000 (the “historical” period) and 2020–2050 (the “future” period). Annual maxima were derived from these “raw” data at grid points near each of the three airports in the urban regions of Washington State (SeaTac, Spokane, and Portland). Statistical significance for differences in distributions was found using the Komolgorov-Smirnov test, for differences in means using the Wilcoxon rank-sum test, and for trends in the entire time series using the Mann-Kendall test, all at a two-sided significance level of 0.05.

Changes in average annual maxima between the two time periods are reported in Table 7. They suggest a likelihood of increasing precipitation intensities at all three locations, although their magnitudes vary considerably for the simulations. Significant changes

were found at SeaTac under both simulations, at Spokane under the ECHAM5/A1B simulation for 24-hour storms, and at Portland under the CCSM3/A2 simulation for 1-hour storms. As in the historical analysis, a breakdown of changes by return period is provided for the 1- and 24-hour durations in Tables 8 and 9, respectively. Curiously, differences at SeaTac and Spokane for shorter duration storms are projected to increase under the CCSM3/A2 simulations but decrease under the ECHAM5/A1B simulations.

A closer inspection of results under the CCSM3/A2 simulations revealed that the vast majority of modeled future annual maxima are projected to occur in the month of November, a finding that was not replicated in the ECHAM5/A1B simulations. Quality control checks demonstrated that these elevated November projections are indeed present in the underlying GCM, but that they originated from the one ensemble member with the greatest divergence from the ensemble mean, which indicates more modest increases in autumn precipitation. Thus, these particular results must be interpreted as the combined influence of systematic climate change and internal climate variability. For a more complete discussion, see Salathé et al. (2009, this report).

In order to use the simulations to generate realistic estimates of future runoff, the raw model output for both periods were bias-corrected and statistically downscaled (“BCSD”) to match the rainfall record at the SeaTac Airport precipitation gauge, as described in Section 4.2. The resulting sequence of hourly precipitation was then used as input to a continuous hydrological model to simulate runoff extremes in two urban watersheds in the central Puget Sound region (Section 5).

## 4.2 Bias correction and statistical downscaling (BCSD)

Although the raw output from the RCM provides a broadly recognizable pattern of rainfall, even a cursory comparison of simulated and gauged records shows obvious disparities in both the frequency of rainfall events and the total amount of recorded precipitation. For example, from 1970 to 2000, the CCSM3/A2 simulation at the grid center closest to SeaTac Airport resulted in 11,734 hours of nonzero precipitation for a total of 225 inches during the month of January (annual averages of 379 hours and 7.3 inches), while the gauges at SeaTac recorded 4144 hours of nonzero precipitation for a total of 162 inches (annual averages of 134 hours and 5.2 inches). The need to remove systematic bias in RCM output has been explored by Wood et al. (2002) and Payne et al. (2004), who described the framework that was used to perform the bias correction used here, refined to be applicable to precipitation extremes. For this analysis we focused on only one region of Washington State, the central Puget Sound region, and we bias-corrected the simulated data month-by-month (rather than on an annual basis) to ensure that the dramatic seasonal differences that characterize rainfall in western Washington were preserved and represented accurately.

Bias correction was applied to the simulation record for the grid point from each of the two downscaled hourly WRF time series (1970–2000 and 2020–2050) that was closest to SeaTac Airport (Figure 4). For the RCM run forced by the CCSM3/A2 simulation (hereafter referred to as the “CCSM3” run), the grid point employed was 47.525°N, 122.287°W, corresponding to a location about 9 km NNE of SeaTac Airport. For the RCM run forced by the ECHAM5/A1B simulation (hereafter referred to as the

“ECHAM5” run), the grid point employed was 47.500°N, 122.345°W, corresponding to a location about 7 km NNW of SeaTac Airport. For purposes of comparison, a separate bias correction was performed for each run at their next gridpoint to the south; results were very similar and are not reported here.

The bias correction procedure is based on probability mapping as described by Wilks (2006). The underlying principle acknowledges biases in RCM-simulated climate but anticipates that the simulation data may still provide useful signals if interpreted relative to the RCM climatology rather than the observed climatology (Wood et al. 2002). The monthly data for grid nodes were thus corrected so that they had the same probability distributions as the observed data from SeaTac airport, which were the same data used in the historical analyses described in Section 3.

The first step in the bias-correction procedure was to truncate simulated data for the 1970–2000 period so that each month had the same number of nonzero hourly values as the observed data from the SeaTac gauge. This was done to correct for the smooth manner in which the RCM simulates precipitation, which creates an unrealistically high number of miniscule hourly observations (what has been termed the “climate model drizzle problem”). Simulated data for the future period (2020–2050) were similarly truncated, using the same threshold hourly values resulting from matching the number of nonzero past values to that which was observed. Thus, using the example provided above, the 7590 (i.e., 11,734–4144) hours containing the smallest amounts of nonzero precipitation were eliminated from the 1970–2000 simulated record for the month of January, coinciding with a truncation threshold of 0.012 inches

The procedure was performed first for the historical period and then for the future period of each RCM run. In the example of January non-zero rainfall days, any hour during the month of January during the 2020–2050 simulated record with a nonzero precipitation of less than 0.012 inches was eliminated (6824 out of 10,322 hours). This process was repeated for each month. Bias correction was then achieved by replacing RCM values with values having the same nonexceedence probabilities, with respect to the observed climatology, that the original RCM values had with respect to the RCM climatology (where the climatology is defined from the historical period of each data set). Monthly totals were first calculated (by year), and Weibull plotting position was employed to map those totals from the simulated empirical cumulative distribution function (eCDF) to monthly totals from the observed eCDF. Simulated hourly values were then rescaled to add up to the new monthly totals. These new hourly values were then mapped from their eCDF to the hourly values from the observed eCDF, and once again rescaled to add up to the monthly totals derived in the first mapping step. Values that fell outside the range of the simulated climatology, but within 3.5 standard deviations of the climatological mean, were corrected by assuming a lognormal distribution. Those that fell outside of 3.5 standard deviations of the climatological mean were corrected by simply scaling the mean of the observed climatology by its ratio with the mean of the simulated climatology.

Results of the bias-correction procedure were again tested for significance using the Komolgorov-Smirnov, Wilcoxon rank-sum, and Mann-Kendall tests at a two-sided  $\alpha$  of 0.05. Overall, average biases in empirical annual maxima were reduced from -22.2% to

+3.1% for the ECHAM5 run, and from +9.6% to +2.5% for the CCSM3 run (Table 10). Changes in the raw annual maxima between the 1970–2000 and 2020–2050 periods were largely preserved, although the procedure did have the effect of making some of the changes under the CCSM3/A2 simulation more statistically significant. Under the ECHAM5 run, the corrected empirical annual maxima display a decrease between the two 30-year periods by an average of 5.8 to 6.3% for 1-, 2-, and 3-hour durations, and an increase of 2.3 to 14.1% for the remaining durations. Under the CCSM3 run, the corrected empirical annual maxima show an increase of 13.7 to 28.7% across all durations. Time series of 24-hour annual maxima resulting from the bias-corrected data are plotted alongside those resulting from observed data in Figure 5. As shown, the means and ranges of the simulated data generally match those of the observed data from 1970 to 2000. The plots illustrate the wide interannual variation in annual maxima, which is not well captured in summary statistics like changes in means.

The results from our analysis of historical precipitation trends (Section 3) affirm an increase in the intensity of extreme events in the Seattle-Tacoma area. The magnitude of observed increases for the 24-hour storm over the past 50 years (24.7%) is comparable to the magnitudes of projected increases for the same duration over the next 50 years (14.1 to 28.7%, depending upon the data employed), all of which are statistically significant to some degree. This has potential implications for stormwater management, which is explored more directly in the next section.

## 5. Prediction of future changes in urban flood extremes

Although our historical analysis focused on changes in precipitation across major urban areas of Washington State, the direct relevance of these changes to stormwater infrastructure is best displayed through predictions of future streamflows. As case studies, we selected two Seattle-area watersheds (Figure 4), Thornton Creek in the City of Seattle and Juanita Creek in the City of Kirkland and adjacent unincorporated King County, because they encompass physical and land-use characteristics typical of the central Puget Lowland. The Thornton Creek watershed is Seattle's largest watershed, with approximately 28.7 km<sup>2</sup> (11.1 mi<sup>2</sup>) of mixed commercial and residential land use. Juanita Creek is a mixed-land-use 17.6 km<sup>2</sup> (6.8 mi<sup>2</sup>) watershed that drains to the eastern shore of Lake Washington; its land cover is 34% effective impervious with 30% forest cover.

Hydrologic simulations of streamflows in these two watersheds were generated by the Hydrologic Simulation Program-Fortran (HSPF; Bicknell et al. 1996). HSPF, which was developed under contract to and is maintained by the U.S. Environmental Protection Agency, is a lumped-parameter model that simulates discharge at user-selected points along a channel network from a time series of meteorological variables (notably, rainfall, temperature, and solar radiation) and a characterization of hydrologic variables (such as infiltration capacity and soil water-holding capacity) that are typically averaged over many hectares or square kilometers. HSPF has enjoyed widespread application across western Washington since its first regional application in the mid-1980s (King County

1985), and the procedures for model set-up, initial parameter selection, and calibration are well established for the region (Dinicola et al. 1990, 2001).

The BCSD precipitation data for the periods 1970–2000 and 2020–2050, using the RCM grid points previously discussed (see Section 4.2; Table 6 and Figure 4), were input to HSPF to reconstitute historical streamflows and predict future streamflows in the Thornton Creek and Juanita Creek watersheds. Since the inputs to the hydrologic model for the two periods differed only in precipitation, any attribute of an altered hydrologic response that is not driven predominantly by rainfall (e.g., the dependence of low-flow extremes on evapotranspiration rates) would not be plausibly represented and have not been explored here. These two case studies, however, offer some guidance on whether predicted runoff changes in urban and suburban areas present any critical areas of concern for stormwater managers.

## **5.1 Results**

To parallel the approach of the BCSD analysis, HSPF was first employed to evaluate differences in 1970–2000 simulated flows as forced by both the historical rainfall record and the BCSD rainfall. Results from both the Thornton Creek and Juanita Creek modeling runs suggest streamflow biases of the same magnitude or less than those from the direct comparison of observed and simulated rainfall records (see Tables 11, 12, 13 and Figure 6). For the exploratory purposes that motivated the modeling, these differences were judged acceptable.

Streamflows were then simulated for both watersheds and each of the two RCM runs using the BCSD rainfall for the periods 1970–2000 and 2020–2050. Log-Pearson Type 3 distributions were fitted to the resulting annual maxima, and changes were tested for statistical significance using the Komolgorov-Smirnov, Wilcoxon rank-sum, and Mann-Kendall tests at a two-sided  $\alpha$  of 0.05. Results at the mouths of both watersheds (Tables 11 and 12) indicate increases in streamflows for both RCM runs and all recurrence intervals. While these increases are more muted at the mouth of Juanita Creek, this is most likely the consequence of an extensive wetlands complex that serves to attenuate peak flows in that watershed.

Despite this relative uniformity, however, not every scenario is equally consistent. Statistically significant results using CCSM3-generated precipitation are systematically greater than those using ECHAM5, which are not significant. In addition, in the HSPF results for Kramer Creek, a 45-ha (120-ac) mixed commercial and residential subwatershed that constitutes less than 2% of the Thornton Creek watershed area, simulated changes in peak flow conflict in sign between the two scenarios. For the CCSM3-driven simulations, 2-yr through 50-yr peak flows are projected to rise by as much as 25% while the ECHAM5-driven simulations mostly indicate small *declines* (Table 13). Although only a single example, these are dramatically different, even contradictory results, suggesting that the present state of understanding is still highly uncertain, at least for small urban drainage basins of this scale.

We have explored predicted changes under both RCM runs for additional flow metrics beyond simply peak annual discharge, using selected indices of hydrologic alteration (IHA) that have likely ecological influence (Konrad and Booth 2002; Richter et al. 1996). These indices are generally grouped into those that assess the time of year for average or extreme flow events, the frequency and duration of flow pulses, and the rate and frequency of change in flow conditions. In general, these metrics did not change between the two modeled time intervals nearly as much as did the peak annual discharge (e.g., Table 11). As an example, the results on Juanita Creek for a “time-of-year” metric, the high pulse start date (Figure 7), are similar to most of the others: only modest differences are apparent between the two scenarios, and very limited differences between the two simulation periods.

In contrast, analysis of a common measure of stream-channel erosivity (aggregate duration of flow above a threshold discharge) displays a suggestion of systematic change between the present and future periods. The threshold discharge assumed in this study is 50% of the peak 2-year flow for the period 1970–2000, a credible index value for initiation of sediment transport in an alluvial gravel-bed channel (Booth and Jackson 1997). A single value, derived from the average of the three 1970–2000 simulations, was used as this “threshold discharge” for all duration analyses at a given stream location. Both GCM-driven simulations show consistent increases, with the largest change associated with the smallest watershed area (Table 14). Similar to other results comparing simulated 2020–2050 flows to those from 1970–2000, increases in erosivity predicted using the CCSM3 precipitation dataset are consistently more dramatic than those predicted using the ECHAM5 dataset. In comparison to streamflow simulation

driven by the historical 1970–2000 rainfall record, however, both GCM-driven simulations consistently over-estimate high-flow durations by approximately one-third. Interestingly, the two different GCM-based simulations produce very consistent errors; apparently the bias-correction procedures does not adequately adjust the moderate levels of precipitation intensity that affect this flow statistic.

## 6. Discussion

Our findings from the analyses of historical precipitation indicate that there have been shifts in the distributions of extreme precipitation events over the past half-century, but with substantial differences in different parts of the state. In the Puget Sound region, statistically significant increases were observed in annual maxima at the 24-hour duration, which is the interval most frequently used for the design of stormwater infrastructure. Annual maxima in the other two regions, however, display markedly different responses over the last 50 years, with mixed results in the Spokane region and consistently negative changes in the Portland-Vancouver region, none of which were statistically significant. Although prior studies have generally focused on trends in the *frequency* of extreme events, and not in *intensity* as we have done here, these results are generally consistent with those of Kunkel et al. (1999) and Pryor et al. (2009), both of which found rather ambiguous trends in the Pacific Northwest, as well as Madsen and Figdor (2007), which found significant upward trends in both Washington and Seattle, but conflicting trends in Oregon and Idaho. Anticipating uniform responses in the patterns of future rainfall across all of Washington State, therefore, is surely

unwarranted—adaptations will need to be region-specific, because historical changes in rainfall are spatially variable even within the western half of the state.

Modeled trends in future extreme precipitation broadly extend the trends of the historical analyses. Two different GCMs provided the coarse-scale simulated climatic data used to generate downscaled precipitation results, and both agree in general trends and overall magnitude. The precise level of rainfall increases predicted by the two models, however, vary significantly, and actual changes may be difficult to distinguish from natural variability. Although the historical analyses suggest that the magnitude of future projected increases is plausible (and, in fact, consistent with past trends), the differences between the two model predictions are sufficiently large to carry significant consequences for their direct application in the design of stormwater facilities.

Nonetheless, the evidence suggests that drainage infrastructure designed using mid-20th century rainfall records may be subject to a future rainfall regime that differs from current design standards.

Results of the hydrologic modeling on two urban watersheds in the central Puget Sound region affirm and extend both the broad trends and the substantial uncertainties evident in the precipitation simulations. For the two modeled watersheds, simulations provide general agreement that peak discharges will increase, although the range of predicted change (from a slight decrease to a near-doubling, depending on the selected recurrence interval, the watershed, and the underlying GCM simulation) are much too large on which to predicate engineering designs. The comparative simulation results are most confounding for the smallest watershed areas, wherein even the net direction of change

(i.e., a future increase or a future decrease) is in part dependent on the choice of GCM model.

In part, these inconsistencies must reflect the inherent limitations of the present generation of downscaled rainfall data—for a small (and even not-so-small) urban watershed, an hourly time step is many times longer than the lag-to-peak of the basin (the time between the maximum rainfall intensity and the maximum stream discharge), and so the rainstorms that give rise to the largest discharges in these flashy systems will be simulated poorly (if at all). However, within-watershed comparisons demonstrate that the differences in the two GCMs, which themselves span only a modest range of the entire ensemble of global climate models, display sufficient variability to preclude their present use as a basis for the design of stormwater facilities.

## 7. Conclusions

- **Few statistically significant changes in extreme precipitation have been observed to date in the state's three major metropolitan areas, with the possible exception of the Puget Sound.** Nonetheless, drainage infrastructure designed using mid-20th century rainfall records may be subject to a future rainfall regime that differs from current design standards.
- **Projections from two regional climate model (RCM) simulations generally indicate increases in extreme rainfall magnitudes throughout the state over**

**the next half-century, but their projections vary substantially by both model and region, and actual changes may be difficult to distinguish from natural variability.**

- **Hydrologic modeling of two urban creeks in central Puget Sound suggest overall increases in peak annual discharge over the next half-century, but only those projections resulting from one of the two RCM simulations are statistically significant.** Magnitudes of projected changes vary widely, depending on the particular basin under consideration and the choice of the underlying global climate model.

## **8. Research Gaps and Recommendations for Future Research**

Our assessment of future streamflows, and the magnitude of peak discharges on which the design of stormwater infrastructure is based, suggest that concern over present design standards is warranted and that some adaptation to changing conditions is already probably prudent (particularly in the Puget Sound region, where regional downscaling and simulations of future streamflow were conducted). However, this analysis is based on just two GCMs and so is at most suggestive. For a more complete understanding of how precipitation extremes are likely to change in the future, the methods employed in the precipitation distribution analysis should be used to explore a larger sample of simulated future climate data. Additional model simulations, based on a larger ensemble of GCMs and emission scenarios, are needed to develop a more robust set of conclusions

and provide additional information for evaluating alternative stormwater-facility design standards.

## **9. Acknowledgments**

This study was conducted under the auspices of the University of Washington's Climate Impact Group, with primary funding received from the Washington State Legislature. Additional support was also provided by Seattle Public Utilities and Northwest Hydraulic Consultants (to DH), King County Water and Land Resources Division (to JB), and Stillwater Sciences (to DBB). We would also like to acknowledge the encouragement and insights of Paul Fleming and Gary Schimek (City of Seattle).

## **10. References**

- Bicknell BR et al. (1996) Hydrological Simulation Program – Fortran: User's manual for Release 11. US Environmental Protection Agency, Environmental Research Laboratory, Office of Research and Development, Athens, Georgia
- Booth DB, Jackson CR (1997) Urbanization of aquatic systems - degradation thresholds, stormwater detention, and the limits of mitigation. *J Am Water Resour Assoc* 22(5)
- Choguill CL (1996) Ten steps to sustainable infrastructure. *Habitat Int* 20(3) 389-404
- Crabbé P, Robin M (2006) Institutional adaptation of water resource infrastructures to climate change in eastern Ontario. *Clim Chang* Doi: 10.1007/s10584-006-9087-5

- Denault C, Millar RJ, Lence BJ (2002) Climate change and drainage infrastructure capacity in an urban catchment. Annual conference of the Canadian Society for Civil Engineering, Montreal, Quebec, Canada
- Dinicola et al. (1990) Characterization and simulation of rainfall-runoff relations for headwater basins in western King and Snohomish Counties, Washington. US Geological Survey Water-Resources Investigation Report 89-4052
- Dinicola et al. (2001) Validation of a numerical modeling method for simulating rainfall-runoff relations for headwater basins in western King and Snohomish Counties, Washington. US Geological Survey Water-Supply Paper 2495
- Efron B (1979) Bootstrap methods: another look at the jack-knife. *Annals of Stat*
- Fowler HJ, Kilsby CG (2003) A regional frequency analysis of United Kingdom extreme rainfall from 1961 to 2000. *Int J Climatol*
- Gerstel WJ, Brunengo MJ, Lingley WS Jr, Logan RL, Shipman H, and Walsh TJ (1997) Puget Sound bluffs: the where, why, and when of landslides following the 1996/97 storms. *Wash Geol* 25(1):17-31
- Groisman PY, Knight RW, Easterling DR, Karl TR, Hegerl GC, Razuvaev VN (2005) Trends in intense precipitation in the climate record. *J Clim* 18(9):1326-1350
- Hamlet AF, Lee SY, Mickleson KEB, Elsner MM (2009) Effects of projected climate change on energy supply and demand in the Pacific Northwest. Washington Climate Change Impacts Assessment: Evaluating Washington's future in a changing climate. In press
- Hanson R (ed) (1984) Perspectives on urban infrastructure. Committee on National Urban Policy, National Research Council, Washington DC. National Academies Press, 216 pp

- Hosking JRM, Wallis JR (1997) Regional frequency analysis: an approach based on L-moments. Cambridge University Press, New York
- Huppert DD, Moore A, Dyson K (2009) Impacts of climate change on the coasts of Washington State. Washington Climate Change Impacts Assessment: Evaluating Washington's future in a changing climate. In press
- Intergovernmental Panel on Climate Change (IPCC) (2007) Climate change 2007: synthesis report. contribution of working groups I, II and III to the fourth assessment report of the Intergovernmental Panel on Climate Change [core writing team Pachauri RK, Reisinger A eds.] Geneva, Switzerland
- Karl TR, Knight RW (1998) Secular trends of precipitation amount, frequency, and intensity in the United States. Bull Am Meteorol Soc
- King County (1985) Juanita Creek basin plan. King County Department of Public Works, Surface Water Management Division, Seattle, Washington
- Kirschen P, Ruth M, Anderson M, Lakshmanan TR (2004) Infrastructure systems, services and climate change: Integrated impacts and response strategies for the Boston metropolitan area. Tufts University: Climate's Long-term impacts on metro Boston (CLIMB). USEPA Grant Number R.827450-01, final report (see <http://www.aia.org/SiteObjects/files/CLIMB%20Executive%20Summary.pdf>). Accessed 6 Dec 2008
- Konrad CP, Booth DB (2002) Hydrologic trends associated with urban development for selected streams in the Puget Sound basin, western Washington. US Geological Survey Water Resources Investigations Report No. 4040
- Kunkel KE, Andsager K, Easterling DR (1999) Long-term trends in extreme precipitation events over the conterminous United States and Canada. J Clim 12:2515-2527

- Kunkel KE, Easterling DR, Redmond K, Hubbard K (2003) Temporal variations of extreme precipitation events in the United States: 1895-2000. *Geophys Res Lett* 30(17):1900
- Larsen P, Goldsmith S (2007) How much might climate change add to future costs for public infrastructure? Institute of Social and Economic Research, University of Alaska Anchorage. UA Research Summary No. 8
- Leopold LB (1968) Hydrology for urban land planning – a guidebook on the hydrologic effects of urban land use. Geological Survey Circular 554
- Leung LR, Kuo YH, and Tribbia J (2006) Research needs and directions of regional climate modeling using WRF and CCSM. *B Am Meteorol Soc* 87:1747-1751
- Lettenmaier DP, Wallis JR, Wood EF (1987) Effect of regional heterogeneity on flood frequency estimation. *Water Resour Res* 23(2): 313-324
- Madsen T, Figdor E (2007) When it rains, it pours: global warming and the rising frequency of extreme precipitation in the United States. Report prepared by Environment America Research and Policy Center, Boston
- Mote P, Salathé E, Peacock C (2005) Scenarios of future climate for the Pacific Northwest. Report prepared by the Climate Impacts Group, Center for Science in the Earth System, Joint Institute for the Study of the Atmosphere and Oceans, University of Washington, Seattle, available at <http://ces.washington.edu/db/pdf/kc05scenarios462.pdf>
- Payne JT et al. (2004) Mitigating the effects of climate change on the water resources of the Columbia River Basin. *Clim Chang* 62(1-3) 233-256

- Pryor SC, Howe JA, Kunkel KE (2009) How spatially coherent and statistically robust are temporal changes in extreme precipitation in the contiguous USA? *Int J Clim* 29:31-45
- Richter BD, Baumgartner JV, Powell J, and Braun DP (1996) A method for assessing hydrologic alteration within ecosystems. *Conserv Biol* 10:1163-1174
- Salathé EP (2005) Downscaling simulations of future global climate with application to hydrologic modeling. *Int J Climatol*
- Salathé EP, Steed R, Mass CF, and Zahn P (2008) A high-resolution climate model for the U.S. Pacific Northwest: Mesoscale feedbacks and local responses to climate change. *J Climate* 21:5708-5726
- Salathé, EP., Y. Zhang, L.R. Leung, Y. Qian. (2009) Regional climate model projections for the State of Washington. *Washington Climate Change Impacts Assessment: Evaluating Washington's Future in a Changing Climate*. In Press.
- Shaw H, Reisinger A, Larsen H, Stumbles C (2005) Incorporating climate change into stormwater design – why and how? *South Pacific Conference on Stormwater and Aquatic Resource Protection*, Ministry for the Environment, Auckland, New Zealand
- Trenberth K, Dai A, Rasmussen RM, Parsons DB (2003) The changing character of precipitation. *Bull Am Meteorol Soc* 84(9): 1205-1217
- Urbonas BR, Roesner LA (1993) Hydrologic design for urban drainage and flood control. In: Maidment DR (ed) *Handbook of hydrology*, McGraw-Hill, New York
- Vano JA, Voisin N, Cuo L, Hamlet AF, Elsner MM, Palmer RN, Polebitski A, Lettenmaier DP (2009a) Multi-model assessment of the impacts of climate change on water management in the Puget Sound region, Washington, USA. *Washington*

- Climate Change Impacts Assessment: Evaluating Washington's future in a changing climate. In press
- Vano JA, Voisin N, Scott M, Stockle CO, Halmet AF, Mickleson KEB, Elsner MM, Lettenmaier DP (2009b) Multi-model assessment of the impacts of climate change on water management and agriculture of the Yakima River basin, Washington, USA. Washington Climate Change Impacts Assessment: Evaluating Washington's future in a changing climate. In press
- Waters D, Watt WE, Marsalek J, Anderson BC (2003) Adaptation of a storm drainage system to accommodate increased rainfall resulting from climate change. *J Environ Plan and Manag* 46(5): 755–770
- Watt WE, Waters D, Mclean R (2003) Climate variability and urban stormwater infrastructure in Canada: Context and case studies. Toronto-Niagara Region Study Report and Working Paper Series, Meteorological Service of Canada, Waterloo, Ontario, Canada
- Wilks DS (2006) Statistical methods in the atmospheric sciences, Second Edition. Academic Press
- Wood AW, Maurer EP, Kumar A, Lettenmaier DP (2002) Long-range experimental hydrologic forecasting for the eastern United States. *J Geophys Res*
- Washington State Department of Transportation (WADOT) (2008) Storm-related closures of I-5 and I-90: Freight Transportation Economic Impact Assessment Report. Washington State Department of Transportation WA-RD 708.1

Table 1. Stations used in the regional frequency analysis.

Region	Station	State	Co-op ID	Reported Period	# of Years Removed	Sample Size
Puget Sound	Blaine	WA	729	1949–2007	7	52
	Burlington	WA	986	1949–2007	5	54
	Centralia 1W	WA	1277	1968–2007	3	37
	Everett	WA	2675	1949–2007	4	55
	McMillin Reservoir	WA	5224	1949–2007	14	45
	Olympia AP	WA	6114	1949–2007	8	51
	Port Angeles	WA	6624	1949–2007	13	46
	Seattle Tacoma AP	WA	7473	1949–2007	0	59
Spokane	Couer d'Alene	ID	1956	1949–2007	20	39
	Dworshak Fish Hatchery	ID	2845	1967–2007	1	40
	Harrington 1 NW	WA	3515	1962–2007	5	41
	Lind 3 NE	WA	4679	1949–2007	5	54
	Plummer 3 WSW	ID	7188	1949–2007	12	47
	Pullman 2 NW	WA	6789	1949–2007	6	53
	Sandpoint Exp Stn	ID	8137	1960–2007	5	43
	Spokane Intl AP	WA	7938	1949–2007	0	59
Vancouver	Colton	OR	1735	1949–2007	2	57
	Cougar 4 SW	WA	1759	1949–2007	3	56
	Goble 3 SW	OR	3340	1949–2007	2	57
	Gresham	OR	3521	1949–2007	9	50
	Longview	WA	4769	1955–2007	10	43
	Portland Intl AP	OR	6751	1949–2007	0	59
	Sauvies Island	OR	7572	1949–2007	1	58

Table 2. Changes in average fitted annual maxima between 1956–1980 and 1981–2005, as determined by the regional frequency analysis at SeaTac, Spokane, and Portland Airports. Kolmogorov-Smirnov (top), Wilcoxon rank-sum (middle), and Mann-Kendall (bottom) p-values are provided in italics. Those p-values found to be significant at a two-sided  $\alpha$  of 0.05 are indicated in bold.

	SeaTac	Spokane	Portland
1-hour	+7.2%	-1.0%	+4.4%
KS	<i>0.877</i>	<i>0.124</i>	<i>0.237</i>
rank-sum	<i>0.547</i>	<i>0.272</i>	<i>0.217</i>
MK	<i>0.192</i>	<i>0.892</i>	<i>0.137</i>
2-hour	+10.0%	-5.2%	-5.3%
KS	<i>0.877</i>	<i>0.649</i>	<i>0.990</i>
rank-sum	<i>0.534</i>	<i>0.409</i>	<i>0.846</i>
MK	<i>0.184</i>	<i>0.800</i>	<i>0.926</i>
3-hour	+14.2%	+0.3%	-6.6%
KS	<i>0.124</i>	<i>0.877</i>	<i>0.414</i>
rank-sum	<i>0.398</i>	<i>0.683</i>	<i>0.491</i>
MK	<i>0.166</i>	<i>0.704</i>	<i>0.404</i>
6-hour	+12.7%	+0.7%	-8.2%
KS	<i>0.649</i>	<i>0.414</i>	<i>0.237</i>
rank-sum	<i>0.438</i>	<i>0.600</i>	<i>0.130</i>
MK	<i>0.199</i>	<i>0.926</i>	<i>0.141</i>
12-hour	+18.7%	+14.9%	-5.2%
KS	<i>0.237</i>	<i>0.237</i>	<i>0.124</i>
rank-sum	<i>0.187</i>	<i>0.151</i>	<i>0.095</i>
MK	<i>0.226</i>	<i>0.070</i>	<i>0.113</i>
24-hour	+24.7%	+6.9%	+1.9%
KS	<i>0.237</i>	<i>0.649</i>	<i>0.414</i>
rank-sum	<i>0.052</i>	<i>0.567</i>	<i>0.332</i>
MK	<i>0.140</i>	<i>0.584</i>	<i>0.302</i>
2-day	+22.3%	+2.9%	-6.6%
KS	<i>0.124</i>	<i>0.990</i>	<i>0.414</i>
rank-sum	<b><i>0.023</i></b>	<i>0.923</i>	<i>0.151</i>
MK	<b><i>0.038</i></b>	<i>0.781</i>	<i>0.185</i>
5-day	+13.4%	-10.1%	-5.0%
KS	<i>0.237</i>	<i>0.124</i>	<i>0.649</i>
rank-sum	<i>0.082</i>	<i>0.146</i>	<i>0.362</i>
MK	<i>0.276</i>	<i>0.161</i>	<i>0.361</i>

10-day	+7.3%	-3.9%	-9.7%
KS	0.124	0.877	0.237
rank-sum	0.146	0.541	0.146
MK	0.303	0.503	0.155

Table 3. Distribution of changes in fitted 1- and 24-hour annual maxima from 1956–1980 to 1981–2005 at SeaTac, Spokane, and Portland Airports. Numbers in italics represent the return periods of the 1981–2005 events that are equal in magnitude to the 1956–1980 events having the return periods indicated in the first column. As an example, for the 1-hour storm at SeaTac, the 25-year event from 1956 to 1980 [having a 4% (1/25) chance of occurring in any given year] became a 16.7-year event from 1981 to 2005 [having a 6% (1/16.7) chance of occurring in any given year]. Average changes across all return periods are provided at the bottom, matching those reported in Table 2, with Kolmogorov-Smirnov (top), Wilcoxon rank-sum (middle), and Mann-Kendall (bottom) p-values provided in italics. None of the changes were found to be significant at a two-sided  $\alpha$  of 0.05.

Return Period (yrs)	1-hour Storm			24-hour Storm		
	SeaTac	Spokane	Portland	SeaTac	Spokane	Portland
2	+3.6% <i>1.8</i>	+7.7% <i>1.7</i>	+3.8% <i>1.8</i>	+22.8% <i>1.4</i>	+8.7% <i>1.6</i>	-2.2% <i>2.1</i>
5	+3.5% <i>4.4</i>	+2.9% <i>4.5</i>	+4.5% <i>4.2</i>	+30.2% <i>2.1</i>	+7.5% <i>3.6</i>	+5.3% <i>4.1</i>
10	+5.8% <i>8.1</i>	-3.1% <i>11.3</i>	+5.0% <i>8.0</i>	+33.3% <i>3.0</i>	+5.9% <i>7.4</i>	+10.3% <i>6.5</i>
25	+11.0% <i>16.7</i>	-12.6% <i>45.0</i>	+5.7% <i>19.0</i>	+35.8% <i>5.3</i>	+3.4% <i>20.4</i>	+16.8% <i>11.8</i>
50	+16.2% <i>27.9</i>	-20.2% <i>140.0</i>	+6.3% <i>36.8</i>	+37.0% <i>8.4</i>	+1.2% <i>46.3</i>	+21.7% <i>18.1</i>
Average	+7.2%	-1.0%	+4.4%	+24.7%	+6.9%	+1.9%
<i>KS</i>	<i>0.877</i>	<i>0.124</i>	<i>0.237</i>	<i>0.237</i>	<i>0.649</i>	<i>0.414</i>
<i>rank-sum</i>	<i>0.547</i>	<i>0.272</i>	<i>0.217</i>	<i>0.052</i>	<i>0.567</i>	<i>0.332</i>
<i>MK</i>	<i>0.192</i>	<i>0.892</i>	<i>0.137</i>	<i>0.140</i>	<i>0.584</i>	<i>0.302</i>

Table 4. Results of the precipitation event analysis from 1949 to 2007. Trends in annual precipitation are provided for the 59-year period as a percentage of the average annual precipitation, as are the portions of these trends due to trends in event frequency and event intensity. Trends in annual median and maximum event intensity are provided as a percentage of their respective long-term averages. Mann-Kendall p-values are provided in italics; none of the trends were found to be significant at a two-sided  $\alpha$  of 0.05. An “event” is defined as any day with measurable (nonzero) precipitation.

	SeaTac	Spokane	Portland
Average annual number of events	154.5	110.2	152.1
Average annual precipitation (in)	38.2	16.5	36.6
Trend in annual precipitation <i>MK</i>	-8.9 % <i>0.219</i>	-13.0 % <i>0.055</i>	-8.3 % <i>0.202</i>
...due to trend in event frequency <i>MK</i>	-9.3 % <i>0.056</i>	-11.9 % <i>0.052</i>	-2.6 % <i>0.843</i>
...due to trend in event intensity <i>MK</i>	+0.4 % <i>0.628</i>	-1.1 % <i>0.433</i>	-5.7 % <i>0.239</i>
Trend in annual median event intensity <i>MK</i>	+4.6 % <i>0.917</i>	-1.4 % <i>0.437</i>	-2.7 % <i>0.420</i>
Trend in annual maximum event intensity <i>MK</i>	+39.0 % <i>0.174</i>	+9.1 % <i>0.527</i>	-2.3 % <i>0.798</i>

Table 5. Results of the exceedance-over-threshold analysis from 1949 to 2007. Trends in the annual number of events exceeding the specified thresholds are provided for the 59-year period as a percentage of the average annual number of respective exceedances. Mann-Kendall p-values are provided in italics; those found to be significant at a two-sided  $\alpha$  of 0.05 are indicated in bold. An “event” is defined as any day with measurable (nonzero) precipitation.

	0.1"	0.2"	0.3"	0.4"	0.5"
SeaTac	-10.9%	-15.0%	-15.8%	-13.1%	-12.4%
<i>MK</i>	<i>0.094</i>	<b><i>0.039</i></b>	<b><i>0.045</i></b>	<i>0.148</i>	<i>0.161</i>
Max	121	87	61	46	39
Min	68	40	25	12	9
Spokane	-14.8%	-15.1%	-21.2%	-23.9%	-17.7%
<i>MK</i>	<b><i>0.022</i></b>	<i>0.123</i>	<i>0.074</i>	<i>0.168</i>	<i>0.244</i>
Max	76	46	27	17	11
Min	38	19	8	2	2
Portland	-4.2%	-8.8%	-13.3%	-16.1%	-18.9%
<i>MK</i>	<i>0.356</i>	<i>0.153</i>	<b><i>0.038</i></b>	<i>0.141</i>	<i>0.187</i>
Max	116	92	69	51	41
Min	65	37	22	14	9

Table 6. Summary of emission scenarios, GCMs, and geographic coordinates of the downscaled precipitation records used for this study.

IPCC Emissions Scenario	Global Circulation Model (GCM)	Regional Climate Model (RCM)	RCM grid spacing for Washington State simulation	Lat-Long Coordinates of RCM output used for hydrologic modeling (see Figure 4)	
A2 <sup>1</sup>	CCSM3	WRF	20 km	47.525°N	122.287°W
A1B <sup>2</sup>	ECHAM5	WRF	36 km	47.500°N	122.345°W

<sup>1</sup>A2 simulations performed by Pacific Northwest National Laboratories

<sup>2</sup>A1B simulations performed by UW-CIG

Table 7. Changes in the average modeled empirical annual maxima from 2020 to 2050 relative to the average modeled empirical annual maxima from 1970 to 2000, using raw RCM data. Kolmogorov-Smirnov (top), Wilcoxon rank-sum (middle), and Mann-Kendall (bottom) p-values are provided in italics. Those p-values found to be significant at a two-sided  $\alpha$  of 0.05 are indicated in bold.

	CCSM3/A2			ECHAM5/A1B		
	SeaTac	Spokane	Portland	SeaTac	Spokane	Portland
1-hour	+16.2%	+10.3%	+10.5%	-4.6%	-6.6%	+2.1%
KS	<b>0.014</b>	0.120	0.120	0.944	0.062	0.363
rank-sum	<b>0.011</b>	0.272	<b>0.044</b>	0.757	0.346	0.714
MK	<b>0.015</b>	0.220	<b>0.004</b>	0.388	0.504	0.183
2-hour	+16.9%	+5.9%	+7.0%	-4.3%	-6.4%	+3.9%
KS	0.062	0.062	0.062	0.944	0.778	0.944
rank-sum	<b>0.013</b>	0.163	0.076	0.811	0.473	1.000
MK	<b>0.027</b>	0.091	<b>0.007</b>	0.362	0.466	0.085
3-hour	+17.5%	+6.3%	+6.5%	-4.0%	-5.8%	+2.9%
KS	<b>0.030</b>	0.120	0.062	0.944	0.560	0.944
rank-sum	<b>0.007</b>	0.128	0.078	0.966	0.456	1.000
MK	<b>0.020</b>	<b>0.044</b>	<b>0.009</b>	0.395	0.416	0.174
6-hour	+18.3%	+5.4%	+3.6%	+3.6%	-1.7%	+1.2%
KS	0.120	0.216	0.062	0.560	0.560	0.998
rank-sum	<b>0.019</b>	0.231	0.147	0.439	0.588	0.966
MK	0.116	0.104	0.055	0.181	0.455	0.388
12-hour	+15.9%	+5.5%	-0.5%	+9.1%	+12.1%	+2.1%
KS	0.216	0.559	0.778	0.217	0.062	0.778
rank-sum	0.076	0.536	0.545	0.121	0.065	0.811
MK	0.331	0.568	0.375	0.106	0.080	0.331
24-hour	+18.7%	+3.9%	+4.8%	+14.9%	+22.2%	+2.0%
KS	0.216	0.778	0.363	<b>0.006</b>	<b>0.013</b>	0.778
rank-sum	0.052	0.944	0.346	<b>0.022</b>	<b>0.023</b>	0.933
MK	0.291	0.875	0.356	<b>0.045</b>	<b>0.049</b>	0.560
2-day	+11.2%	+4.2%	+2.0%	+13.8%	+16.0%	+3.1%
KS	0.120	0.363	0.363	<b>0.030</b>	0.363	0.560
rank-sum	0.143	0.855	0.318	<b>0.034</b>	0.159	0.844
MK	0.331	0.789	0.362	0.072	0.123	0.932

5-day	+6.3%	+3.2%	+9.0%	+12.2%	+8.8%	+4.6%
KS	0.559	0.944	0.120	0.120	0.560	0.944
rank-sum	0.318	0.933	0.181	0.050	0.278	0.833
MK	0.618	0.799	0.114	0.123	0.302	0.585
10-day	+9.0%	+2.3%	+7.5%	+7.2%	+8.9%	+11.5%
KS	0.216	0.944	0.363	0.216	0.120	0.363
rank-sum	0.177	0.704	0.200	0.190	0.200	0.402
MK	0.572	0.971	0.145	0.322	0.229	0.531

Table 8. Distribution of changes in fitted 1-hour annual maxima from 1970-2000 to 2020-2050, using raw RCM data. Numbers in italics represent the return periods of the 1981-2005 events that are equal in magnitude to the 1956–1980 events having the return periods indicated in the first column. Average changes across all return periods are provided at the bottom, matching those reported in Table 7, with Kolmogorov-Smirnov (top), Wilcoxon rank-sum (middle), and Mann-Kendall p-values (bottom) provided in italics. Those p-values found to be significant at a two-sided  $\alpha$  of 0.05 are indicated in bold.

Return Period (yrs)	CCSM3/A2			ECHAM5/A1B		
	SeaTac	Spokane	Portland	SeaTac	Spokane	Portland
2	+16.7% <i>1.3</i>	+6.4% <i>1.7</i>	+15.6% <i>1.3</i>	-1.1% <i>2.1</i>	-8.6% <i>2.6</i>	-0.7% <i>2.0</i>
5	+15.8% <i>2.6</i>	+5.1% <i>4.3</i>	+8.7% <i>3.2</i>	-5.5% <i>6.4</i>	-10.1% <i>7.4</i>	+4.3% <i>4.2</i>
10	+15.2% <i>4.7</i>	+7.1% <i>8.1</i>	+3.3% <i>7.9</i>	-8.9% <i>16.1</i>	-9.2% <i>14.5</i>	+7.9% <i>6.9</i>
25	+14.3% <i>11.1</i>	+12.6% <i>17.5</i>	-3.9% <i>36.3</i>	-13.4% <i>56.8</i>	-6.2% <i>32.0</i>	+13.1% <i>13.1</i>
50	+13.7% <i>21.9</i>	+18.7% <i>30.3</i>	-9.4% <i>149.2</i>	-16.8% <i>153.3</i>	-2.8% <i>55.9</i>	+17.2% <i>20.9</i>
Average	+16.2%	+10.3%	+10.5%	-4.6%	-6.6%	+2.1%
KS	<i><b>0.014</b></i>	<i>0.120</i>	<i>0.120</i>	<i>0.944</i>	<i>0.062</i>	<i>0.363</i>
rank-sum	<i><b>0.011</b></i>	<i>0.272</i>	<i><b>0.044</b></i>	<i>0.757</i>	<i>0.346</i>	<i>0.714</i>
MK	<i><b>0.015</b></i>	<i>0.220</i>	<i><b>0.004</b></i>	<i>0.388</i>	<i>0.504</i>	<i>0.183</i>

Table 9. Distribution of changes in fitted 24-hour annual maxima from 1970–2000 to 2020–2050, using raw RCM data. Numbers in italics represent the return periods of the 2020–2050 events that are equal in magnitude to the 1970–2000 events having the return periods indicated in the first column. Average changes across all return periods are provided at the bottom, matching those reported in Table 7, with Kolmogorov-Smirnov (top), Wilcoxon rank-sum (middle), and Mann-Kendall (bottom) p-values provided in italics. Those p-values found to be significant at a two-sided  $\alpha$  of 0.05 are indicated in bold.

Return Period (yrs)	CCSM3/A2			ECHAM5/A1B		
	SeaTac	Spokane	Portland	SeaTac	Spokane	Portland
2	+13.5% <i>1.4</i>	-4.4% <i>2.3</i>	+9.9% <i>1.6</i>	+20.8% <i>1.3</i>	+15.3% <i>1.5</i>	-3.1% <i>2.2</i>
5	+13.1% <i>3.2</i>	-2.8% <i>5.5</i>	+5.9% <i>3.7</i>	+18.5% <i>2.3</i>	+28.7% <i>2.2</i>	+1.9% <i>4.6</i>
10	+16.7% <i>5.4</i>	+3.1% <i>9.0</i>	+1.5% <i>8.9</i>	+13.7% <i>4.4</i>	+38.5% <i>3.0</i>	+7.3% <i>7.1</i>
25	+24.3% <i>9.9</i>	+15.0% <i>14.9</i>	-4.8% <i>46.9</i>	+5.9% <i>14.5</i>	+52.1% <i>4.2</i>	+16.0% <i>11.3</i>
50	+32.1% <i>14.9</i>	+27.0% <i>20.4</i>	-9.5% <i>335.4</i>	-0.5% <i>53.0</i>	+63.0% <i>5.3</i>	+23.6% <i>15.1</i>
Average	+18.7%	+3.9%	+4.8%	+14.9%	+22.2%	+2.0%
<i>KS</i>	<i>0.216</i>	<i>0.778</i>	<i>0.363</i>	<b><i>0.006</i></b>	<b><i>0.013</i></b>	<i>0.778</i>
<i>rank-sum</i>	<i>0.052</i>	<i>0.944</i>	<i>0.346</i>	<b><i>0.022</i></b>	<b><i>0.023</i></b>	<i>0.933</i>
<i>MK</i>	<i>0.291</i>	<i>0.875</i>	<i>0.356</i>	<b><i>0.045</i></b>	<b><i>0.049</i></b>	<i>0.560</i>

Table 10. Results of the bias-correction procedure for both RCM runs at SeaTac. The reported biases are those of the average modeled empirical annual maxima (both raw and corrected) relative to the average observed empirical annual maxima from 1970 to 2000. The reported changes are those of the average modeled empirical annual maxima from 2020 to 2050 relative to the average modeled empirical annual maxima from 1970 to 2000, using both raw and corrected data. Kolmogorov-Smirnov (top), Wilcoxon rank-sum (middle), and Mann-Kendall (bottom) p-values are provided in italics. Those p-values found to be significant at a two-sided  $\alpha$  of 0.05 are indicated in bold.

	CCSM3/A2				ECHAM5/A1B			
	Bias		Change		Bias		Change	
	Raw	Cor	Raw	Cor	Raw	Cor	Raw	Cor
1-hour			+16.2%	+14.3%			-4.6%	-6.3%
KS			<i><b>0.014</b></i>	<i><b>0.002</b></i>			<i>0.944</i>	<i>0.944</i>
rank-sum	-19.2%	-7.3%	<i><b>0.011</b></i>	<i><b>0.013</b></i>	-33.2%	-13.4%	<i>0.757</i>	<i>0.554</i>
MK			<i><b>0.015</b></i>	<i><b>0.003</b></i>			<i>0.388</i>	<i>0.799</i>
2-hour			+16.9%	+22.8%			-4.3%	-5.8%
KS			<i>0.062</i>	<i><b>0.001</b></i>			<i>0.944</i>	<i>0.998</i>
rank-sum	-2.6%	+4.1%	<i><b>0.013</b></i>	<i><b>0.001</b></i>	-21.2%	+3.9%	<i>0.811</i>	<i>0.612</i>
MK			<i><b>0.027</b></i>	<i><b>0.001</b></i>			<i>0.362</i>	<i>0.623</i>
3-hour			+17.5%	+23.7%			-4.0%	-6.3%
KS			<i><b>0.030</b></i>	<i><b>0.002</b></i>			<i>0.944</i>	<i>0.778</i>
rank-sum	+2.4%	+6.2%	<i><b>0.007</b></i>	<i><b>0.000</b></i>	-17.3%	+11.8%	<i>0.966</i>	<i>0.573</i>
MK			<i><b>0.020</b></i>	<i><b>0.001</b></i>			<i>0.395</i>	<i>0.536</i>
6-hour			+18.3%	+24.3%			+3.6%	+2.3%
KS			<i>0.120</i>	<i><b>0.030</b></i>			<i>0.560</i>	<i>0.363</i>
rank-sum	+8.8%	+6.6%	<i><b>0.019</b></i>	<i><b>0.005</b></i>	-17.3%	+12.8%	<i>0.439</i>	<i>0.508</i>
MK			<i>0.116</i>	<i><b>0.044</b></i>			<i>0.181</i>	<i>0.185</i>
12-hour			+15.9%	+24.2%			+9.1%	+8.3%
KS			<i>0.216</i>	<i><b>0.030</b></i>			<i>0.217</i>	<i>0.216</i>
rank-sum	+12.7%	+4.4%	<i>0.076</i>	<i><b>0.009</b></i>	-20.6%	+6.8%	<i>0.121</i>	<i>0.151</i>
MK			<i>0.331</i>	<i>0.155</i>			<i>0.106</i>	<i>0.080</i>

24-hour			+18.7%	+28.7%			+14.9%	+14.1%
KS	+11.0%	-1.9%	0.216	<b>0.013</b>	-22.7%	+3.4%	<b>0.006</b>	0.062
rank-sum			0.052	<b>0.003</b>			<b>0.022</b>	<b>0.040</b>
MK			0.291	0.085			<b>0.045</b>	<b>0.034</b>
2-day			+11.2%	+24.0%			+13.8%	+14.1%
KS	+19.4%	-1.1%	0.120	<b>0.013</b>	-22.7%	+1.2%	<b>0.030</b>	<b>0.006</b>
rank-sum			0.143	<b>0.004</b>			<b>0.034</b>	<b>0.023</b>
MK			0.331	0.099			0.072	<b>0.033</b>
5-day			+6.3%	+13.7%			+12.2%	+11.5%
KS	+29.0%	+7.1%	0.559	0.216	-22.4%	+1.1%	0.120	0.062
rank-sum			0.318	0.069			0.050	0.054
MK			0.618	0.437			0.123	0.072
10-day			+9.0%	+18.0%			+7.2%	+7.8%
KS	+25.1%	+4.6%	0.216	<b>0.002</b>	-22.4%	+0.3%	0.216	0.216
rank-sum			0.177	<b>0.010</b>			0.190	0.168
MK			0.572	0.078			0.322	0.193
Average	+9.6%	+2.5%	-	-	-22.2%	+3.1%	-	-

Table 11. Comparisons of HSPF-simulated annual maximum streamflows at the mouth of Juanita Creek, as forced by bias-corrected data for 1970–2000 and 2020–2050 from each of the two RCM runs. Percent differences indicated are with respect to HSPF-simulated annual maximum streamflows as forced by observed data for 1970–2000. Kolmogorov-Smirnov (top), Wilcoxon rank-sum (middle), and Mann-Kendall (bottom) p-values are provided in italics at bottom, with those p-values found to be significant at a two-sided  $\alpha$  of 0.05 indicated in bold.

Return Interval (yrs)	CCSM3-WRF				ECHAM5-WRF			
	Peak Flow Quantiles 1970-2000 (cfs)	% Diff with Obs	Peak Flow Quantiles 2020-2050 (cfs)	Change From 1970-2000	Peak Flow Quantiles 1970-2000 (cfs)	% Diff with Obs	Peak Flow Quantiles 2020-2050 (cfs)	Change From 1970-2000
2	230	+6%	289	+25%	224	+3%	252	+13%
5	285	+3%	358	+25%	287	+4%	318	+11%
10	318	+1%	400	+26%	330	+4%	358	+9%
25	358	-3%	451	+26%	383	+4%	405	+6%
50	386	-5%	488	+26%	424	+4%	438	+3%
KS rank-sum MK				<i><b>0.030</b></i> <i><b>0.002</b></i> <i><b>0.040</b></i>				<i>0.216</i> <i>0.147</i> <i>0.056</i>

Table 12. Comparisons of HSPF-simulated annual maximum streamflows at the mouth of Thornton Creek, as forced by bias-corrected data for 1970–2000 and 2020–2050 from each of the two RCM runs. Percent differences indicated are with respect to HSPF-simulated annual maximum streamflows as forced by observed data for 1970–2000. Kolmogorov-Smirnov (top), Wilcoxon rank-sum (middle), and Mann-Kendall (bottom) p-values are provided in italics at bottom, with those p-values found to be significant at a two-sided  $\alpha$  of 0.05 indicated in bold.

Return Interval (yrs)	CCSM3-WRF				ECHAM5-WRF			
	Peak Flow Quantiles 1970-2000 (cfs)	% Diff with Obs	Peak Flow Quantiles 2020-2050 (cfs)	Change From 1970-2000	Peak Flow Quantiles 1970-2000 (cfs)	% Diff with Obs	Peak Flow Quantiles 2020-2050 (cfs)	Change From 1970-2000
2	118	+17%	187	+58%	107	+6%	134	+25%
5	186	+14%	292	+57%	173	+6%	225	+30%
10	238	+10%	364	+53%	227	+5%	296	+30%
25	312	+6%	458	+47%	309	+5%	399	+29%
50	373	+2%	529	+42%	381	+5%	485	+27%
KS rank-sum MK				<b>0.003</b> <b>0.001</b> <b>0.005</b>				<i>0.951</i> <i>0.624</i> <i>0.399</i>

Table 13. Comparisons of HSPF-simulated annual maximum streamflows at the mouth of Kramer Creek, as forced by bias-corrected data for 1970–2000 and 2020–2050 from each of the two RCM runs. Percent differences indicated are with respect to HSPF-simulated annual maximum streamflows as forced by observed data for 1970–2000. Kolmogorov-Smirnov (top), Wilcoxon rank-sum (middle), and Mann-Kendall (bottom) p-values are provided in italics at bottom, with those p-values found to be significant at a two-sided  $\alpha$  of 0.05 indicated in bold.

Return Interval (yrs)	CCSM3-WRF				ECHAM5-WRF			
	Peak Flow Quantiles 1970-2000 (cfs)	% Diff with Obs	Peak Flow Quantiles 2020-2050 (cfs)	Change From 1970-2000	Peak Flow Quantiles 1970-2000 (cfs)	% Diff with Obs	Peak Flow Quantiles 2020-2050 (cfs)	Change From 1970-2000
2	7.0	+4%	8.8	+25%	6.6	-1%	6.7	+3%
5	8.6	+4%	10.6	+24%	8.3	0%	8.3	0%
10	9.5	+1%	11.7	+22%	9.4	0%	9.3	-2%
25	10.6	0%	12.8	+20%	10.9	+3%	10.4	-5%
50	11.4	-1%	13.5	+19%	12.0	+4%	11.2	-7%
KS rank-sum MK				<b>0.001</b> <b>0.001</b> <b>0.001</b>				<i>0.951</i> <i>0.898</i> <i>0.455</i>

Table 14. Flow durations for  $Q > 50\%$  of the 2-year discharge (percent of time exceedance), as predicted by HSPF at four locations along the channel network of Thornton Creek. The first column gives the time of exceedance using the historical record; the “1970–2000” column under each GCM shows the same metric using the BCSD simulated record (with simulation results about 1/3 higher, on average). The column labeled “Change” is the 2020–2050 value for this metric relative to the 1970–2000 durations using the BCSD rainfall record.

<b>SeaTac Historical</b>	<b>CCSM3-WRF</b>			<b>ECHAM5-WRF</b>		
<b>1970-2000</b>	<b>1970- 2000</b>	<b>2020-2050</b>	<b>Change</b>	<b>1970-2000</b>	<b>2020-2050</b>	<b>Change</b>
<b>Kramer Creek (0.45 km<sup>2</sup>)</b>						
0.23%	0.28%	0.58%	+107%	0.29%	0.51%	+76%
<b>South Branch Thornton Creek</b>						
0.23%	0.28%	0.42%	+50%	0.29%	0.34%	+17%
<b>North Branch Thornton Creek</b>						
0.36%	0.45%	0.66%	+47%	0.46%	0.56%	+22%
<b>Thornton Creek nr Mouth (28.7 km<sup>2</sup>)</b>						
0.19%	0.24%	0.38%	+58%	0.24%	0.30%	+25%

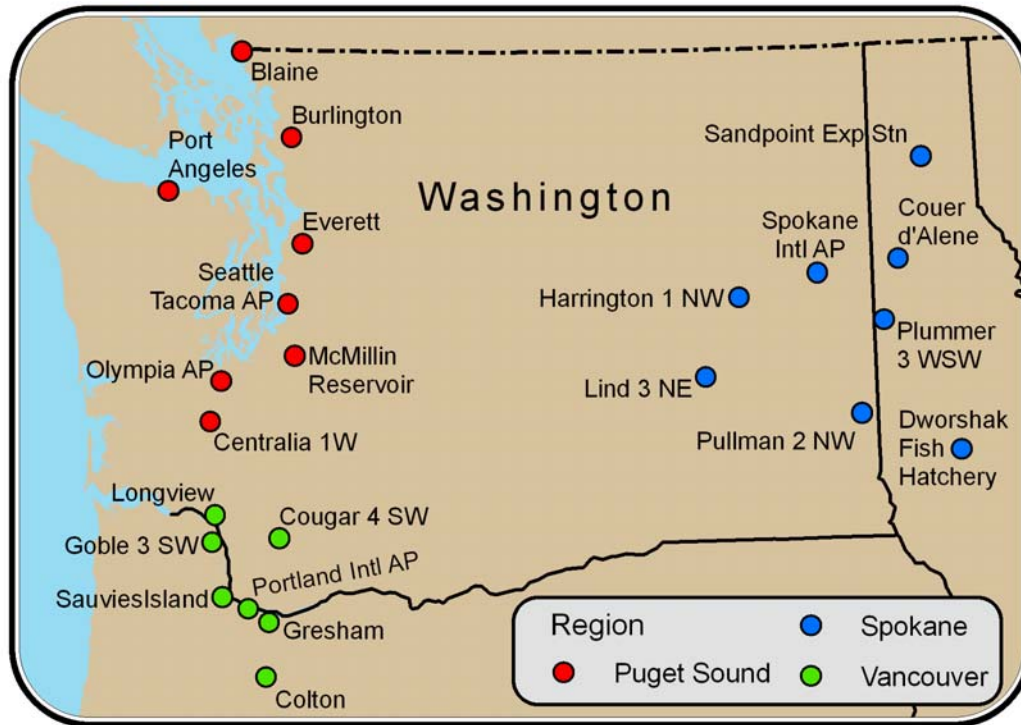


Figure 1. Locations of weather stations used in the regional frequency analysis, grouped by region.

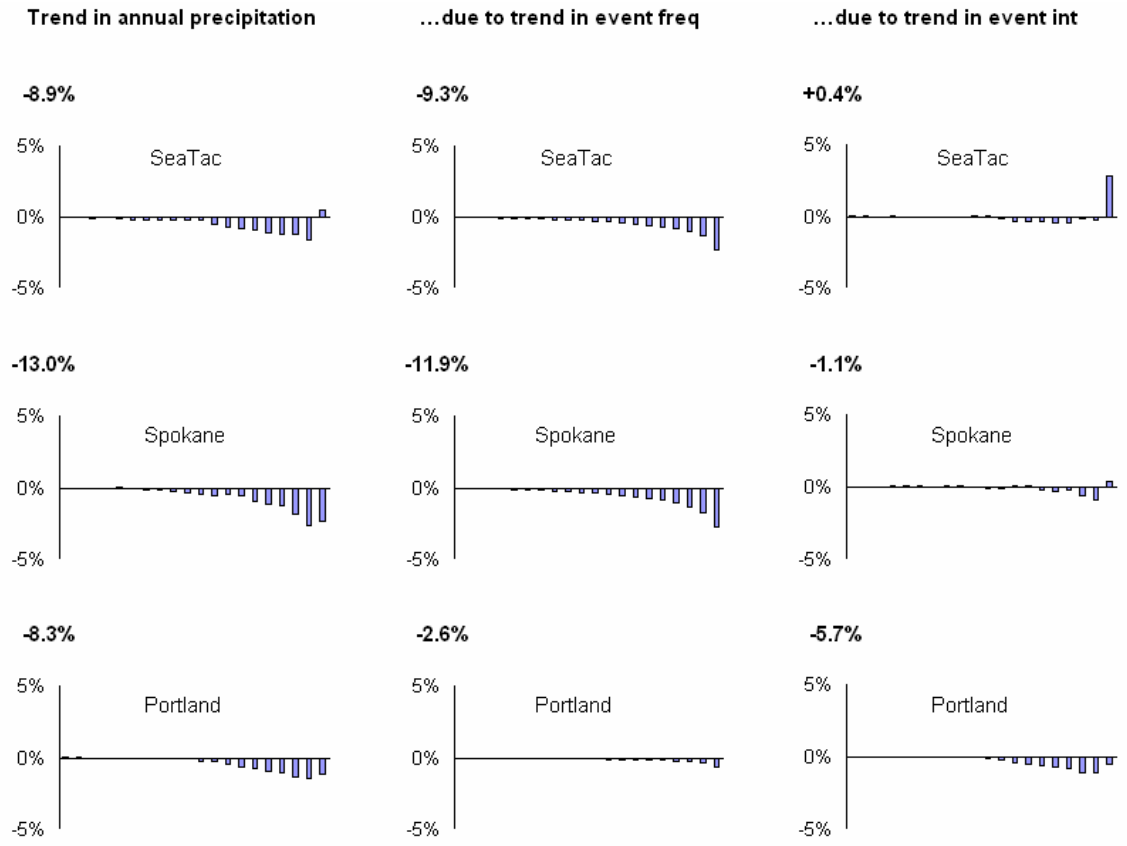


Figure 3. Distribution of trends reported in Table 4. At left are trends in annual precipitation; at center, the portion of the trends in annual precipitation due to trends in event frequency; at right, the portion of the trends in annual precipitation due to trends in event intensity. An “event” is defined as any day with measurable (nonzero) precipitation. Trends for individual class intervals are represented by the bars in each graph, with the class interval containing the smallest 5% of events at left and the class interval containing the largest 5% of events at right. Values above each graph show cumulative trends across all 20 class intervals.



Figure 4. Locations of the two gridpoints used for BCSD, shown in relation to SeaTac Airport and the Thornton Creek and Juanita Creek watersheds (see Section 5).

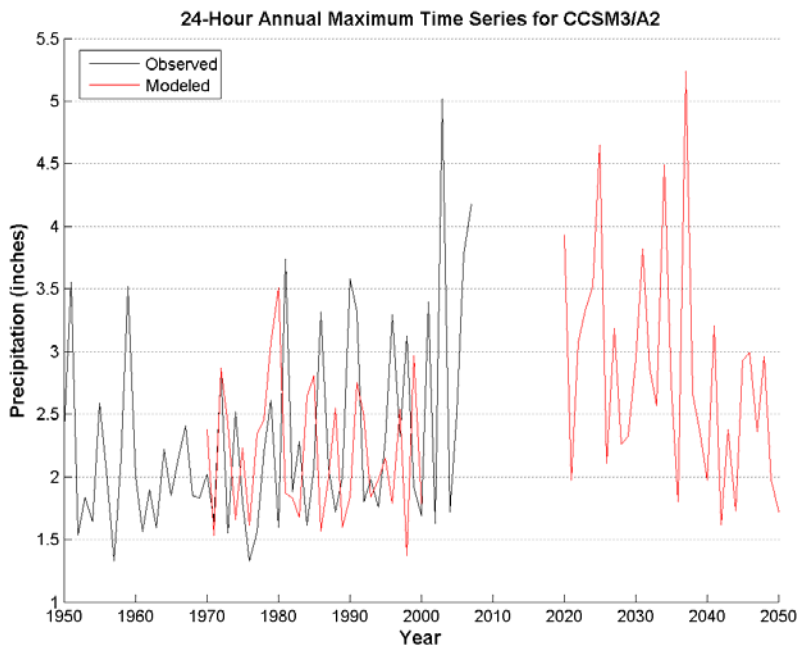
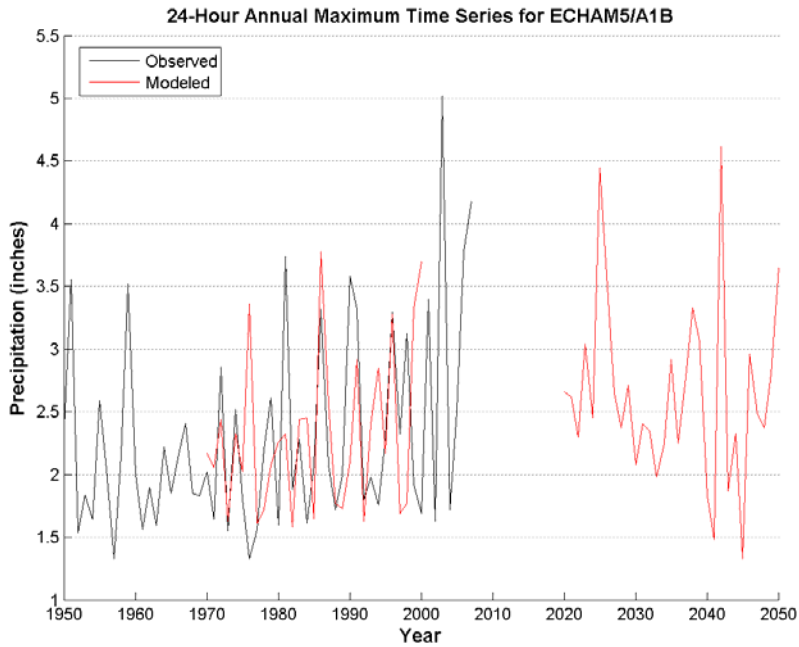


Figure 5. 24-hour annual maxima resulting from the bias-corrected data plotted on top of 24-hour annual maxima resulting from the observed data at SeaTac. As shown, the ranges and means of the simulated data generally match those of the observed data for the historical period (1970–2000).

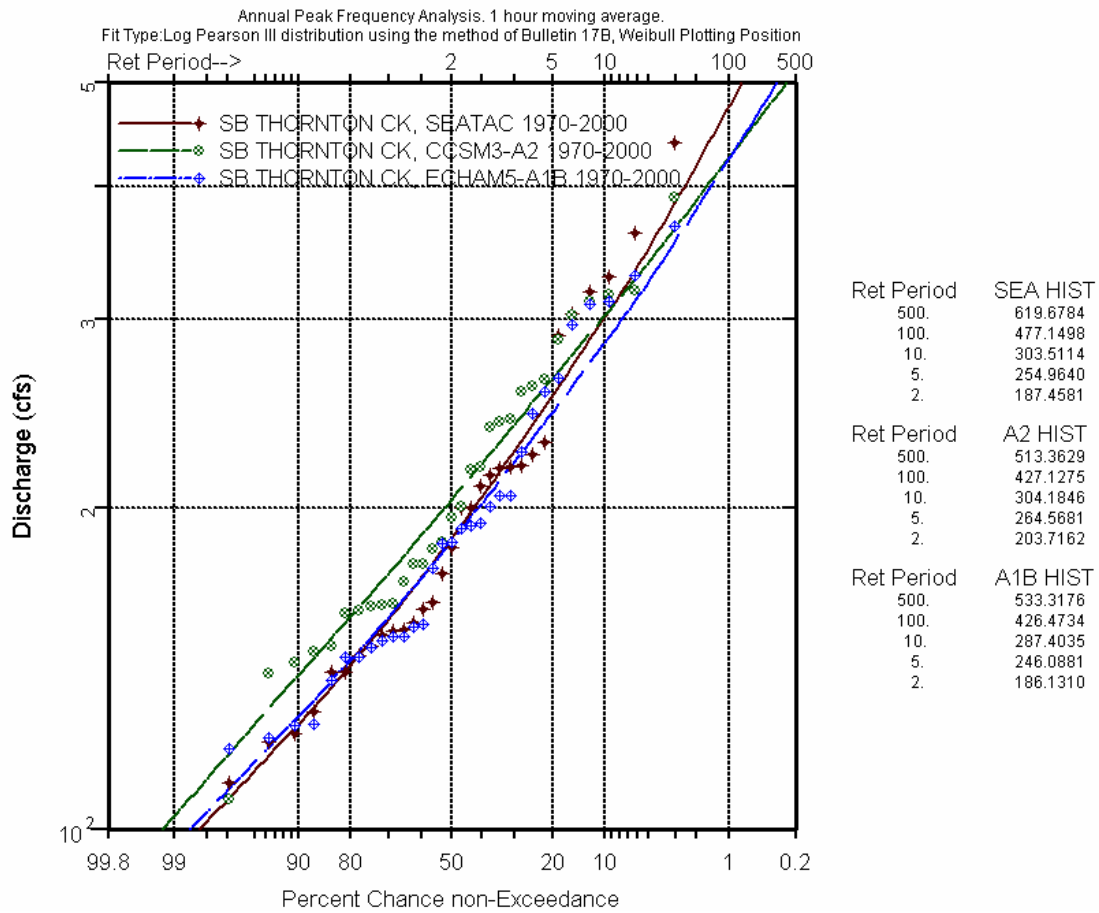


Figure 6. Example Flood Frequency Curves for the South Branch Thornton Creek (930-ha drainage area), comparing HSPF-simulated results for the period 1970–2000 driven by the SeaTac rainfall record (red line and symbols) with the results driven by the BCSD rainfall from the two alternative climate scenarios (green and blue).

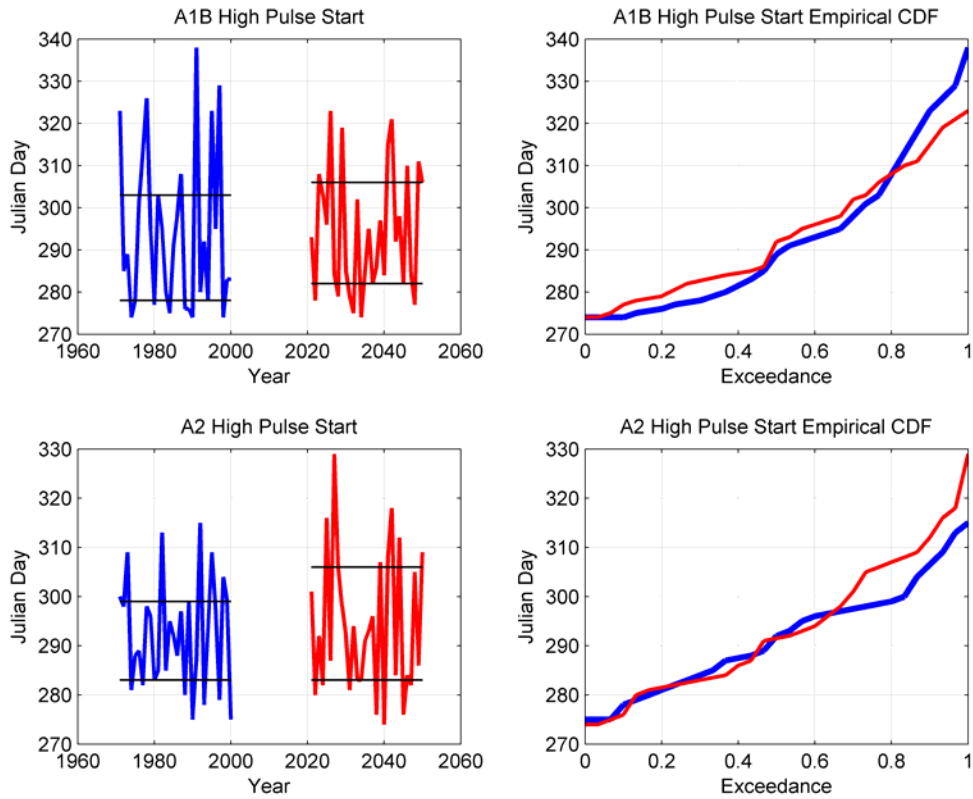


Figure 7. Example of an IHA metric (High Pulse Start Date) as simulated by the two GCM/emission scenarios for the periods 1970–2000 and 2020–2050 at the mouth of Juanita Creek. Differences between models, or between periods, are neither systematic nor particularly large.